Vol. 659: 219–236, 2021
https://doi.org/10.3354/meps13581

MARINE ECOLOGY PROGRESS SERIES
Mar Ecol Prog Ser

Published February 4

Biogeophysical influence of large-scale bathymetric habitat types on mesophotic and upper bathyal demersal fish assemblages: a Hawaiian case study

Astrid Brigitta Leitner[1,2,*], Tobias Friedrich[2], Christopher D. Kelley[2], Seth Travis[2], Dale Partridge[3], Brian Powell[2], Jeffrey C. Drazen[2]

[1]Monterey Bay Aquarium Research Institute, Moss Landing, CA 95039, USA
[2]Department of Oceanography, University of Hawai'i, Mānoa, Honolulu, HI 96822, USA
[3]Plymouth Marine Laboratory, Prospect Place, Plymouth PL1 3DH, UK

ABSTRACT: Seamounts, pinnacles, and crests are abrupt seafloor features that modify physical processes and ecological patterns. Fishers often target these local bathymetric highs, which can have high catch-per-unit-effort. Increases in the abundance of target species has been qualitatively noted around these features and promontories, however, a quantitative evaluation of local highs as preferred habitat for fishes is still lacking. Here, we used an extensive database of fish abundances (N = 2381) from mesophotic and upper bathyal depths (40–300 m) gathered over 8 yr around the Main Hawaiian Islands to evaluate the effects of macro-scale habitat categorized by combining bathymetric position index (BPI) and slope. A numerical model simulating physical ocean processes was used to test the hypothesis that local highs, herein called crests, are distinct and preferred habitat for many species due to their modified flow conditions. We show that crests host a unique, diverse fish assemblage with double the abundance relative to other habitats. Therefore, fishes are concentrated at crests rather than being uniformly distributed along the island shelf at preferred depths. These habitats are characterized by enhanced current amplitudes and convergence zones. Direct correlations between fish abundance, convergence, and current amplitude strongly suggest that flow-enhanced food availability is likely the driver of habitat-related changes in fish assemblage. These results have important implications for conservation and management. We identify a simple and informative method to classify habitat, quantitatively link bathymetry-induced flow alterations to fish abundances, and provide information for refining definitions of essential fish habitat for species that are important commercial targets worldwide.

KEY WORDS: Baited camera · ROMS · Habitat association · Pinnacle · Mesophotic · Bathyal · Bathymetry

1. INTRODUCTION

Sharp gradients in bathymetry can have a significant impact on the dynamics of the ocean. Steep slopes dissipate or convert tidal energy and play an important role in global heat distribution and energy balance by influencing ocean mixing through the generation of internal waves, the dissipation of internal wave energy, and the dissipation of turbulent energy (e.g. Lueck 1997, Rudnick et al. 2003, Friedrich et al. 2011). Bathymetric highs like seamounts, banks, and ridges are some of the most ubiquitous seafloor features on our planet (Wessel et al. 2010, Harris et al. 2014; note that in some papers these are referred to as topographic highs). Global censuses estimate there are between 10s of 1000s and 100000 large

*Corresponding author: aleitner@mbari.org

Publisher: Inter-Research · www.int-res.com

seamounts and banks globally (Wessel et al. 2010), in addition to the mid-ocean ridge system, which extends over 6.7 million km^2 (Harris et al. 2014). Such bathymetric highs are important ecological habitats that can host diverse, high biomass communities and can be valuable economic resources in terms of fisheries and minerals (Pitcher et al. 2007, Sutton et al. 2008, Morato et al. 2010). Bathymetric lows like canyons and trenches can funnel and accumulate organic matter due to their geomorphology, orientation, location, and modification of current flow patterns, likewise supporting unique and high biomass communities (Vetter & Dayton 1999, Genin 2004, De Leo et al. 2010, Jamieson et al. 2011, Ichino et al. 2015). Even flat, plain habitats have been shown to be distinct benthic habitats with unique communities in the abyssal ocean (Durden et al. 2015, Morris et al. 2016).

The extent of and the scales at which species respond to bathymetry are active areas of research. Many resources are invested in habitat modeling, because understanding and defining essential habitat for individuals or groups of species is key in crafting effective ecosystem-based management plans (Moore et al. 2016, Oyafuso et al. 2017). As ocean mapping technologies advance and habitat databases grow, the trend in this research has been to focus on increasingly finer scales of habitat, even to the meter and sub-meter scales (Kelley et al. 2006, Moore et al. 2009, Oyafuso et al. 2017). While fine-scale habitat associations can be ecologically significant, especially for certain smaller, vulnerable species that require small-scale habitat complexity to hide, larger-scale associations can also be important, especially to larger, more mobile animals (Kelley et al. 2006). These larger-scale associations are more practical to consider for conservation and management purposes. Furthermore, understanding larger-scale habitat associations can provide an interesting opportunity to study the mechanisms that shape fish distributions across habitats at various scales.

The mechanisms responsible for driving differences among bathymetric habitat types are still largely unknown and poorly understood; however, topographic steering and modification of ocean currents are often identified as potential drivers (Genin 2004, Turnewitsch et al. 2013, Ichino et al. 2015). The Main Hawaiian Islands (MHI) make an ideal case study for investigating fish distributions across variable bathymetry and identifying the underlying physical and ecological mechanisms at work. The Hawaiian Islands contain an impressive range of bathymetric habitats: seamounts, pinnacles, crests, flat terraces, slope habitats, channels, valleys, and canyons. Hawai'i also has an economically and culturally valuable bottomfish fishery, which mainly targets species of deepwater snappers (lutjanids), jacks (carangids), and groupers (serranids) (Haight et al. 1993a). These families are commercially targeted throughout the Indo-Pacific and globally. In response to the overfishing of several of these important stocks, Hawai'i's Department of Aquatic Resources (DAR) created a system of restricted fishing areas in 1998 and invested in research on the life history and ecology of these species (Parke 2007). The resulting investigations, as well as local fisher lore, suggest that bathymetric habitat types may play an important role in structuring the fish assemblage. Fishers state that offshore pinnacles and seamounts make the best fishing grounds, and qualitative observations from submersible studies support the idea that headlands and bathymetric highs are fish abundance hotspots (Brock & Chamberlain 1968, Kelley et al. 2006). It has been hypothesized, but not yet tested, that this pattern may be driven by bathymetrically enhanced currents that increase local food delivery or nutrient flux, increasing production (Brock & Chamberlain 1968, Ralston et al. 1986, Kelley et al. 2006, Oyafuso et al. 2017).

The goal of this study was to test the importance of large-scale bathymetric habitat types (crests, slopes, flats, and depressions) at mesophotic and upper bathyal depths on demersal fishes in Hawai'i. We specifically tested for effects on fish abundance, diversity, and assemblage composition. Additionally, we relate our findings to an analysis of modeled bottom current structure, with the goal of providing the first quantitative test for the idea that demersal fish distribution patterns are influenced by near bottom current-flow characteristics.

2. MATERIALS AND METHODS

For this study, we focused on bottomfish essential fish habitat (EFH), defined as the 0–400 m depth range surrounding the MHI. High-resolution (i.e. 5 m) multibeam bathymetry and backscatter syntheses exist for the entire habitat area, and local fisheries monitoring programs have resulted in a large database of deepwater fish observations (Smith 2016, Oyafuso et al. 2017, Sackett et al. 2017, Richards et al. 2019, Pacific Islands Fisheries Science Center 2020). For the purposes of this paper, we use the term 'deepwater' as shorthand for referring to the depth range in our database (40–400 m), which spans the mesophotic

zone and extends into the upper bathyal zone (200–1000 m). Additionally, a great deal of effort has gone into successfully parameterizing the Regional Ocean Modeling System (ROMS) in this region (Partridge et al. 2019), as detailed below in Section 2.7. This makes the MHI an ideal study area in which to test the hypothesis that large-scale habitat features influence the local fish assemblage by modifying flow characteristics. In particular, we focused on crests, as bathymetric highs whose mean elevations are relatively higher than the surrounding neighborhood (see Section 2.2 for details). Due to the bathymetry of the MHI, the category 'crests' encompasses both elongated highs, often representing the edge of the island shelf break or ridges, as well other isolated local highs known as pinnacles. In this work, we analyzed both the broad 'crest' category as well as the 2 subcategories (island crest and pinnacle) individually. Specifically, we tested the idea that crests have a higher abundance of fish, a higher diversity, and a unique composition of fish species, and that these distribution patterns are linked to changes in mean current direction and magnitude.

2.1. Fish observations

The observational data used in this study stem from an 8 yr (2007–2015) fishery-independent monitoring program using a baited stereo-video drop-camera system, called BotCam (Merritt et al. 2011). The system was designed to sample the 7 commercially valuable demersal species that include 6 eteline snappers (Lutjanidae): the deepwater red snapper *Etelis carbunculus*, the deepwater longtail red snapper *E. coruscans*, the crimson jobfish *Pristipomoides filamentosus*, the lavender jobfish *P. sieboldii*, the oblique-banded snapper *P. zonatus*, and the rusty jobfish *Aphareus rutilans*; as well as one endemic grouper (Serranidae): the Hawaiian grouper *Hyporthodus quernus*. Collectively, these fish are referred to locally as the Deep 7 or bottomfish (Oyafuso et al. 2017). BotCam also films other members of the larger demersal assemblage at depths between 40 and 300 m. Detailed descriptions of the BotCam system specifications, data collection protocols, sampling scheme, and annotation methods have been previously described (Misa et al. 2013, 2016, Moore et al. 2013, Sackett et al. 2014, 2017). In short, the geometrically calibrated pair of ultra-lowlight cameras was deployed at a height of 3 m above the seafloor for ~40 min. This configuration resulted in a broad enough field of view so that demersal species both in contact with the seafloor and swimming above it were visible. The bait, 800 g of chopped and frozen squid *Loligo opalescens* and anchovy *Engraulis mordax*, is very similar to that used by commercial fishers in chum ('palu') bags to attract these bottomfishes to their hooks. The bait was placed in a plastic mesh canister that remained in the field of view of both cameras. BotCam locations followed a random stratified sampling plan detailed in Misa et al. (2013), which aimed to sample both protected and unprotected areas across hard/soft and high/low sloped habitats. In total, this program collected video from 2381 individual deployments for a total of over 1500 recording hours across the MHI (Fig. 1); however, we excluded a subset of deployments that were only annotated for certain target species, leaving 2271 deployments

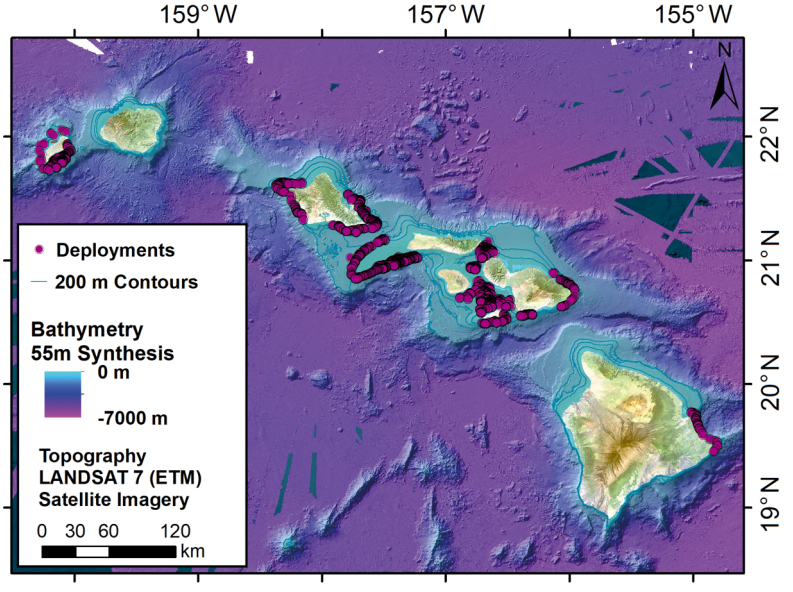

Fig. 1. The 2271 BotCam deployment locations across the Main Hawaiian Islands (MHI). Each maroon circle marks a single deployment. Bathymetry is displayed with a stretched color scale, with turquoise representing the shallowest depths (0 m) and purple representing the deepest values (–6100 m). Depth contours are superimposed in blue at 200 m intervals for depths between 0 and 600 m. The data comes from the Main Hawaiian Island Bathymetric Data Synthesis data set developed by the Hawai'i Mapping Research Group (http://www.soest.hawaii.edu/HMRG/cms/). For the purposes of this figure, the 55 m resolution synthesis (rather than the 5 m resolution) is displayed due to its greater spatial extent. Topography of the MHI comes from the LANDSAT 7 satellite imagery mosaic available through the State of Hawai'i Office of Planning (http://planning.hawaii.gov/)

with annotations for all visible species. During video annotations, fish were identified to the lowest possible taxonomic level, and relative abundances were conservatively estimated for each phylogenetic level (from teleost to species) using the MaxN metric. MaxN is the maximum number of individuals from one taxonomic group visible in a single video frame, and this metric is a standard for conservatively estimating relative abundances from baited video (Priede et al. 1994, Cappo et al. 2006, Misa et al. 2016).

2.2. Habitat classification

The habitat available across the entire MHI was classified using the 5 m resolution bathymetry synthesis generated by the NOAA and the University of Hawai'i (Richards et al. 2019). This bathymetry is freely available from the Hawai'i Mapping Research Group's website (www.soest.hawaii.edu/HMRG/multibeam/bathymetry.php). All habitat classification was done in ArcGIS 10.4 (ESRI) using Benthic Terrain Modeler (Lundblad et al. 2006, Wright et al. 2012).

Bathymetric habitat types were classified based on slope and bathymetric position index (BPI). Slope was classified at a scale of 5 m and given numerical values accordingly (1 = flat: ≤5°; 2 = sloped: >5° following Kelley et al. 2006) to differentiate flat habitats from the others. BPI is a relative position index where the mean elevation at a user-specified area around each point (inner neighborhood) is compared with the mean elevation of a user-specified outer neighborhood (Lundblad et al. 2006). Positive values indicate local highs like crests or pinnacles, and negative values indicate depressions or low points. However, BPI cannot distinguish between flats and constant slopes, thus requiring a combination with slope data. BPI was calculated using a 1250 m scale factor (broad-scale; BBPI) in order to characterize the habitat at the 'mega-scale' (Kelley et al. 2006). The 1250 m scale factor was visually determined to be the most suitable scale factor, able to identify the full range of sizes of pinnacles across the MHI. BBPI was then standardized (sBBPI) following the protocol in Lundblad et al. (2006) and reclassified and scored according to an index value: highs (sBBPI ≥ 150) = 9, neutrals (−50 ≤ sBBPI < 150) = 4, lows (sBBPI < −50) = 1. Summing the slope and sBBPI scores resulted in 6 preliminary categories: flat depression (summed score = 2), steep depression (summed score = 3), flat (summed score = 5), slope (summed score = 6), flat crest (summed score = 10), and steep crest (summed score = 11). These were combined into general habitat types: depression (scores 2 and 3), flat (score 5), slope (score 6), and crest (scores 10 and 11) (Fig. 2, Fig. S1 in the Supplement at www.int-res.com/articles/suppl/m659p219_supp.pdf). We chose to subsequently divide the crest category in order to evaluate if pinnacles and island crests had different effects on fish populations. The crest category was split by manually identifying the elongated island crests and renaming all non-contiguous, isolated features as pinnacles (see Fig. 2). All subsequent analyses that refer to general habitat types group these 2 together under the category 'crest', while those that refer to detailed habitat types differentiate between the subcategories pinnacles and island crests.

2.3. Statistical analysis

In order to determine the influence of bathymetric habitat types on the demersal fish assemblage, we modeled total fish abundance and diversity metrics (species richness, evenness, and Simpson diversity) across the general and detailed habitat categories. Generalized linear mixed models (GLMMs) were used in order to take into account the sampling design. Random effects were included for island, year, month, season, and annotation method, which varied slightly over the course of the 8 yr data set. In addition to the habitat categories, protection sta-

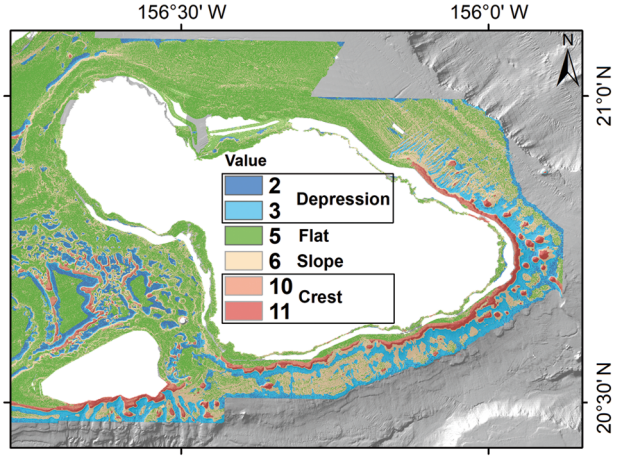

Fig. 2. Habitat classification scheme output for the island of Maui for 0–500 m depths. For maps of all other islands, see Fig. S1. Blues: local lows or depressions (classification scores 2 and 3); green: flat habitats (classification score 5); yellow: slopes (classification score 6); reds: local highs or crests (classification scores 10 and 11) and include both isolated pinnacles and island shelf crests, the long continuous highs at the edge of the island shelf

tus (inside or outside restricted fishing area) and depth, which have both been shown to have an important structuring effect on several of the commercially important demersal species in this region (Kelley et al. 2006, Misa et al. 2013, Oyafuso et al. 2017, Sackett et al. 2017), were also included as fixed effects in the models. Temperature data is highly correlated with depth, so the 2 terms were never included in a single model simultaneously. Models were evaluated by examination of residuals for homogeneity, normality, and independence, and final models were selected using Akaike's information criterion (AICc) calculated with the R package 'MuMIn' (Barton 2016). Significance of predictors were evaluated both using the standard p-value cut-off of $p < 0.05$ and using a ΔAICc metric, such that a ΔAICc value greater than 3 resulting from the removal of a single predictor was taken as significant (Zuur et al. 2010). All statistical analyses were performed within the R statistical environment, version 4.0.2 (R Core Team 2020); see Table 1 for summaries of the final models.

2.4. Model of fish abundance

MaxN of teleosts was compared across habitat types to test the hypothesis that crests supported higher numbers of fish than other habitat types. A negative binomial distribution was chosen for the GLMM due to the high frequencies of zeroes (21%) and low numbers in the database. Across the data set there were 5 outliers, due to large schools of fish, that skewed the normality of the residuals. When these 5 were removed, residuals were patternless and approximately normal, but significance levels remained unchanged, and coefficient values for the predictors of interest were not radically altered.

2.5. Assemblage diversity

Several diversity metrics were used to test whether assemblage diversity changed significantly across habitat types. Species richness was modeled using a model identical to the negative binomial GLMM described above, however, no outliers needed to be removed. Following methods in Chao et al. (2014), we compared rarefied and extrapolated species richness, as well as Shannon and Simpson diversity, which take relative abundances into account (Chao et al. 2014, Hsieh et al. 2016). Confidence intervals were calculated with bootstrap methods and used to evaluate the significance of diversity differences between habitat types (for full details see Chao et al. 2014). Pielou's evenness and Simpson's diversity index were also investigated; however, because these metrics range from 0–1, beta regression models were fit for each with only fixed effects (Cribari-Neto & Zeileis 2010). Models using Simpson diversity and Shannon diversity yielded similar results.

2.6. Assemblage composition

Fish assemblage composition was examined across habitat types. Both the species- and genus-level data contained a large number of zeros. Neither a zero-inflated negative binomial GLMM nor a 2-step hurdle negative binomial GLMM were capable of adequately modeling the data. Both models produced skewed, patterned, non-normal residuals. Therefore, we instead opted for a multivariate approach to determine whether assemblage composition differed significantly with habitat type.

Assemblage analyses used only the most frequently observed species and genera, and these were determined from natural breaks in the MaxN histograms. For the species-level data, 20 species were identified as most frequent, corresponding to those seen in more than 1.5% of 2271 deployments. For genus-level data, the 22 most frequently observed genera were analyzed, again corresponding to a threshold of 1.5% of deployments. The PERMANOVA method, by means of the function 'adonis()' from the R package 'vegan', was used to test the hypothesis that assemblages significantly differed across habitat type (Oksanen et al. 2015). First, the genus and species assemblage data were each converted to a Bray-Curtis dissimilarity matrix, and then one PERMANOVA was completed for species-level assemblage data, and a second was completed for the genus-level data. The same set of predictor variables was used for each analysis (habitat type, depth, protection status, island, month, year). The significance of these predictors was then evaluated using permutation tests. To get marginal tests for each predictor, we repeated each PERMANOVA analysis multiple times, each time using a different predictor as the final variable. Because terms are added sequentially in a PERMANOVA, each of these repeated analyses gives a marginal significance test for the last predictor in the model (Zuur et al. 2010). This allowed for a rigorous evaluation of the significance of each predictor variable.

Where PERMANOVA identified significant habitat effects on assemblage composition, SIMPER was

used to identify the species or genera responsible. Finally, a principal coordinate analysis (PCoA via the capscale function in the R package 'vegan') with a marginal permutation test was used to visualize habitat assemblage differences identified with PERMANOVA and SIMPER. PCoA allows for visual and quantitative assessment of the compositional differences between habitat groups by finding the axes of variation along which the assemblages are most different from each other and mapping the species and sites in this space (Oksanen et al. 2015).

2.7. ROMS

In order to test the idea that fish distribution patterns across habitat types were affected by current flows modified by bathymetric variations, we implemented a high-resolution ROMS model of a subset of our MHI study area (Fig. 3). ROMS version 3.7 (https://www.myroms.org/projects/src) was used to simulate the physical ocean conditions around the island of Ni'ihau. This model domain was chosen because it is relatively isolated from the other islands and contains all habitat types of interest (including the largest pinnacles in the MHI) within a small, manageable spatial extent.

ROMS is a free surface, hydrostatic, primitive equation model with a stretched *s*-coordinate system in the vertical dimension to follow the underwater terrain. ROMS uses a split-explicit time stepping scheme to allow for the barotropic solution to be computed with a much smaller time step than the baroclinic. For this study, the model was configured as per previous Hawaiian studies (Matthews et al. 2012, Janeković et al. 2013, Azevedo Correia de Souza & Powell 2017, Powell 2017, Wong-Ala et al. 2018, Partridge et al. 2019). This includes tidal forcing from TPXO (Egbert & Erofeeva 2002), third-order upstream advection scheme, and a terrain-following *s*-level vertical discretization that distributes the majority of the layers in the upper 250 m of the water column and bottom 50 m. Full details on the model can be found online (www.myroms.org) and in Shchepetkin & McWilliams (2003, 2005).

The Ni'ihau model domain covers the area of 21.65–22.13° N and 160.35–159.94° W with a hori-

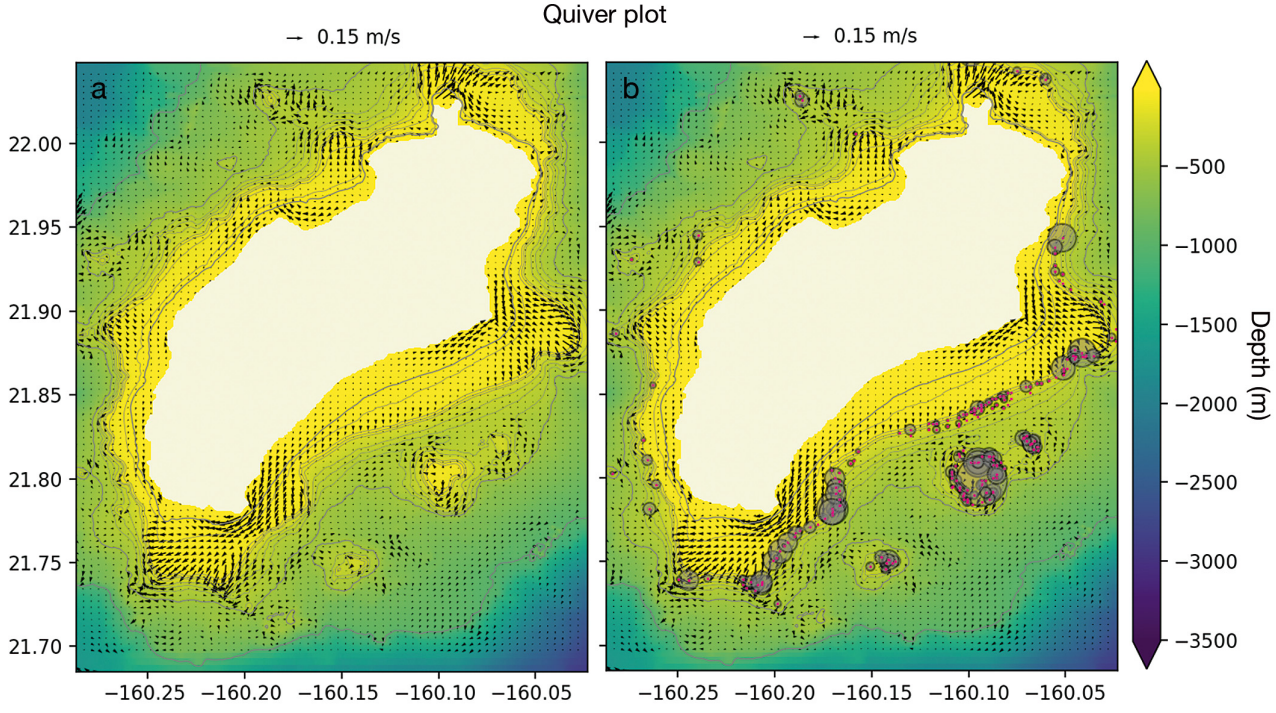

Fig. 3. Maps showing 50 m resolution input bathymetry data (www.soest.hawaii.edu/HMRG/multibeam/bathymetry.php) overlaid with mean current vectors (only every 4th value displayed for clarity) from the ROMS output for the bottom layer for the entire model domain around the island of Ni'ihau. Exposed landmass is in beige. Latitude is plotted on the *y*-axis in °N; longitude on the *x*-axis in °E. Plot color is scaled to depth in meters. Light gray depth contours run from −400 to −50 m by 50 m intervals. Bolded contours mark −1000, −500, and −40 m. (a) Only current vectors are shown (note: arrow length is proportional to flow speed). (b) BotCam deployments locations (pink) overlaid where transparent grey circles around each point are scaled to the teleost MaxN (conservative relative total fish abundance)

zontal resolution of approximately 1/730 degrees (~150 m) and 24 layers (*s*-levels) in the vertical and is configured to provide a higher vertical resolution in shallower waters. The bathymetry for the domain was from the same source as described above but at coarser 50 m resolution to facilitate the current model computations (www.soest.Hawaii.edu/HMRG/multibeam/bathymetry.php). The Ni'ihau domain or grid is nested within the outer model grid of the MHI as described in Partridge et al. (2019). A sponge layer of 12 grid cells linearly increases the viscosity by a factor of 5 and diffusivity by a factor of 1.7 close to the boundary; this effectively acts to reduce boundary effects on the edge of the domain (Partridge et al. 2019). Domain boundary conditions and atmospheric forcing are provided by a 10 yr reanalysis of the Pacific Islands Ocean Observing System (PacIOOS) Hawaiian Island Ocean Forecast System detailed in Partridge et al. (2019). The atmospheric forcing of the model was provided by the Weather Research and Forecasting (WRF) model that is used as part of PacIOOS to make daily predictions (www.pacioos.Hawaii.edu/weather/model-wind-Hawaii/#about). Tidal constituents included in this simulation are the 8 main harmonics: M_2, S_2, N_2, K_2, K_1, O_1, P_1, Q_1, as well as 2 long-period and one non-linear constituent: M_f, M_m, and M_4. To avoid any long-term drifting of the tidal phases related to tidal constituents that were not included in the simulation, the tidal harmonics are updated each year. The model was run for 2 yr with the first 10 d of data discarded to allow for the model to stabilize.

Time-averaged (2 yr) zonal (u) and meridional (v) current speeds were calculated for each grid cell. Bottom current speeds were also calculated for each grid cell at each timestep from u and v:

$$\text{Speed} = \sqrt{u^2 + v^2} \quad (1)$$

Bottom speeds were then time averaged (2 yr) and extracted for all BotCam deployments. Convergence was also calculated for the model domain because both strong- and weak-swimming plankton accumulate where flow compresses and/or converges (Franks 1992, Genin et al. 2005). Higher level predators are attracted to these regions of accumulated prey (Polovina et al. 2001, Genin et al. 2005, Gove et al. 2019). Converging flow can be formed both by compression and convergence of horizontal flows (Franks 1992) and so is defined here with the equation of continuity:

$$\text{Convergence} = -\left(\frac{\delta u}{\delta x} + \frac{\delta v}{\delta y}\right) = \frac{\delta w}{\delta z} \quad (2)$$

Positive convergence values represent converging flows, and negative values represent diverging flows. Because convergence is calculated here for the bottom current, it is analogous to vertical motion ($\delta w/\delta z$) such that areas where bottom flow converges will be areas of upward vertical motion, and areas of divergence will necessarily be areas of downward vertical acceleration. At the bottom boundary, this downward vertical acceleration means that water from above is pulled down into diverging flow at the seafloor. High-density zooplankton patches resulting from behavioral responses to vertical flows have been observed in various oceanographic settings and shown to influence predator distributions (Genin et al. 2005, Benoit-Bird et al. 2013, Gove et al. 2019).

Additionally, mean bottom current amplitude at the tidal frequency (henceforth referred to as current amplitude) was calculated to test the hypothesis that fish are responding primarily to tidal flows. Current amplitude also influences the distribution and patterning of nutrients and prey fields by influencing prey accumulation, dilution, and advection (Pingree et al. 1975, Franks 1992). To calculate current amplitude, current speed was first bandpass-filtered using a Blackman filter to half width frequencies between 6 and 12 h to isolate the tidal signal. Twice the mean absolute value of this filtered tidal signal was taken as the total mean bottom current amplitude at the tidal frequency.

Finally, the relationship between these modeled current parameters and fish abundance was tested statistically with negative binomial GLMMs. Current parameters were extracted for each BotCam deployment location within the model domain (n = 219) using the interpolated value for a radius of 70 m around the drop location in order to incorporate current data from more than one model grid cell in all cases without transitioning to a different habitat type. For these statistical models, the current predictors were rescaled to be centered around 0 in order to account for the large range of scales among the predictors. Correlated variables were removed with an iterative variance inflation factor (VIF) routine such that the predictor with the highest VIF was removed until all VIFs were below 3 (Zuur et al. 2010). All possible models using this list of predictors were then compared and ranked with AICc (dredge function in the R package 'MuMIn') (Barton 2016). The final reported model was the model with the highest degrees of freedom (the most included predictors) within the equivalent best models (those whose ΔAICc were within 2 points from the lowest scoring model).

3. RESULTS

3.1. Fish observations

In total, we observed 42 families of which jacks (Carangidae) and snappers (Lutjanidae) were the most frequent. These 2 families were observed in about 56% of deployments. The next most frequently observed families were groupers (Serranidae), surgeonfishes (Acanthuridae), and requiem sharks (Carcharhinidae), each in around 9% of deployments.

This data set contained observations of 86 genera, 43% of which were rare, appearing in 5 or fewer deployments. *Seriola* and *Pristipomoides* were the most commonly observed genera (in 54 and 38% of deployments, respectively), followed by *Etelis* in 24% of deployments. Rarity of observations was even more pronounced at the species level, where 55 of 112 species appeared in less than 5 deployments (n = 55). *S. rivoliana* was the most commonly recorded species, observed in 40% of deployments, with *P. filamentosus* observed in 30%, and *S. dumerili* in 26%, of deployments. Complete species list and rankings (abundance and presence) can be found in Table S1.

3.2. Fish abundance

Greater abundance and proportions of fishes were observed on higher bathymetric features. From summary statistics alone, 67% of the 112 observed species were most abundant on crests, with 46% on island crests and 21% on pinnacles (Table S2). For the remaining species, 17% were most abundant on slopes and 12 and 4% on flats and depressions, respectively. Deployments with no observed species occurred most commonly in depressions. Fish abundances were also statistically modeled using MaxN of all teleosts as the response variable (Table 1).

Relative abundances of fish varied with some of the factors we investigated. MaxN decreased with depth of deployment ($p < 0.001$), meaning that the shallowest deployments generally had higher numbers of fish. Protection status did not significantly influence fish abundance, possibly due to the large amounts of non-target species included in the analysis. Differences in year, month, island, and season were accounted for in the model with random effects, but significance tests for the random effects were not conducted. The variance of these terms was generally small, but year showed the greatest variance.

Large-scale habitat type was a highly significant predictor of teleost abundance ($p < 0.001$, ΔAICc =

Table 1. Final statistical models. The table is split by the 2 major questions each model addresses. Firstly, what is the influence of bathymetric habitat type on each of 3 different response metrics: species richness, abundance (total teleost MaxN), and composition of the fish assemblage. NB: the fish assemblage model (PERMANOVA with marginal permutation test) was based on a Bray-Curtis dissimilarity matrix calculated from the MaxN of the most abundant species only. The second major question addressed the influence of current flow characteristics and habitat together. Note that flow data was only available for the subset of data around the island of Ni'ihau. Significance of fixed effects are denoted as: $'p < 0.1$, $^{*}p < 0.05$, $^{**}p < 0.01$, $^{***}p < 0.001$. Terms with no identifying markers were not significant. The family column represents the error distribution and link function used in each model

Question	Response	Model type	Family	Predictors	
				Fixed effects	Random effects
Habitat	Richness	GLMM	Negative binomial (log)	MeanTemp*** + Protection$'$ + DetailedHabitat**	(1 | Analysis) + (1 | Island) + (1 | Year) + (1 | Season) + (1 | months)
	Total fish abundance	GLMM	Negative binomial (log)	MeanTemp*** + Protection + DetailedHabitat**	(1 | Analysis) + (1 | Island) + (1 | Year) + (1 | Season) + (1 | months)
	Dissimilarity matrix of top species	PERMANOVA	–	DetailedHabitat*** +Analysis + MeanTemp + Island** + Protection + Project + Season + months + Year$'$	–
Current and habitat	Total Ni'ihau fish abundance	GLMM	Negative binomial (log)	Convergence* + Avg_speed* + MeanDepth*** + Protection*** + DetailedHab***	(1 | Analysis)

109.02, increase of 109.2 points with removal of habitat predictor). Crest habitats had higher relative fish abundances than all other habitats, and when dividing crests into the subcategories of pinnacles and island crests, differences between them were small (Fig. 4). Non-overlapping 95% confidence intervals (represented in Fig. 4 by notches) provided strong evidence for differing medians between all habitat types except pinnacles and island crests (Chambers et al. 1983). In fact, the model predicted nearly twice the relative fish abundance on crests and over twice on pinnacles compared to flats. In contrast, slope habitats were similar to flats with about 1.1 times as many fish as flats, and depressions had the lowest fish abundance (MaxN ~ 0.7). Therefore, we have found strong evidence for the hypothesis that crests support more abundant fish assemblages relative to other types of bathymetry.

3.3. Assemblage diversity

Species richness differed significantly across habitat types (ΔAICc = 133, $p < 0.001$), but Pielou's evenness did not. Slopes and crests had significantly higher species richness than flats and depressions (in increasing order, $p < 0.001$; Fig. S2). Species richness also declined significantly with depth and increased with temperature (depth and temperature are highly correlated: corr = −0.95). Protection status was not found to influence species richness significantly, likely due to the fact that the majority of the species sampled are not targeted by fishers. Diversity as estimated by the Simpson diversity index (incorporates both richness and evenness) was higher ($p < 0.001$) on crests compared to depressions and flats but was not significantly different than slopes.

Because differences in sample size were not accounted for in this analysis, we also compared diversity among habitat types using species richness estimators. Crests and slopes had similar diversities for all metrics, and for species richness, slopes had slightly (<5 at ES25000 — estimated species richness at 25 000 individuals observed) more species than crests although the 95% confidence intervals overlapped (Fig. 5a). When distinguishing pinnacles from island crests, pinnacles actually had a much lower extrapolated species richness than island crests or slopes (ES1296 = 42 vs. 52, and 55, respectively), though still significantly higher than either flats or depressions (ES1296 = 25 and 37, respectively). In comparing diversity indices (Shannon-Wiener diversity index and Simpson diversity index), slopes and crests were still significantly higher than flats and depressions, with slopes having a slightly higher estimated diversity (Fig. 5b,c). When separating the 2 classes of crests, pinnacle diversity (both Shannon and Simpson diversity) was so much lower than either slope or island crest diversity that the confidence bands overlapped those for flats and depressions (Fig. 5d). Across the diversity metrics, crests and slopes hosted a greater number of species compared to flats and depressions.

3.4. Assemblage composition

Geomorphological habitat types were found to support significantly different assemblages of demersal fishes. The assemblage compositions of the different habitat types were found to be significantly different (PERMANOVA, $p < 0.001$), with both marginal permutational significance tests (see Section 2.6) and single predictor models. The species responsible for driving at least 80% of the differences between habitats were *P. filamentosus*, *E. carbunculus*, *E. coruscans*, *P. sieboldii*, *S. rivoliana*, *S. dumerili*, and *Squalus mitsukurii*. *Aphareus rutilans* and *Symphysanodon typus* were only important for the slope/crest pair. The most

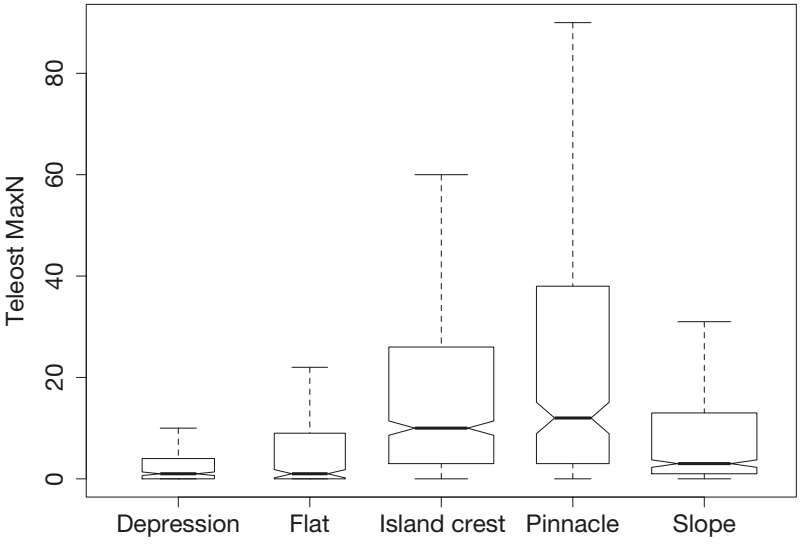

Fig. 4. Total fish abundance (Teleost MaxN) among different habitat types. Center line: median; lower and upper hinges: 25th and 75th percentiles; upper whisker extends from the upper hinge to 1.5 × the interquartile range; notches: 95% confidence intervals around the medians

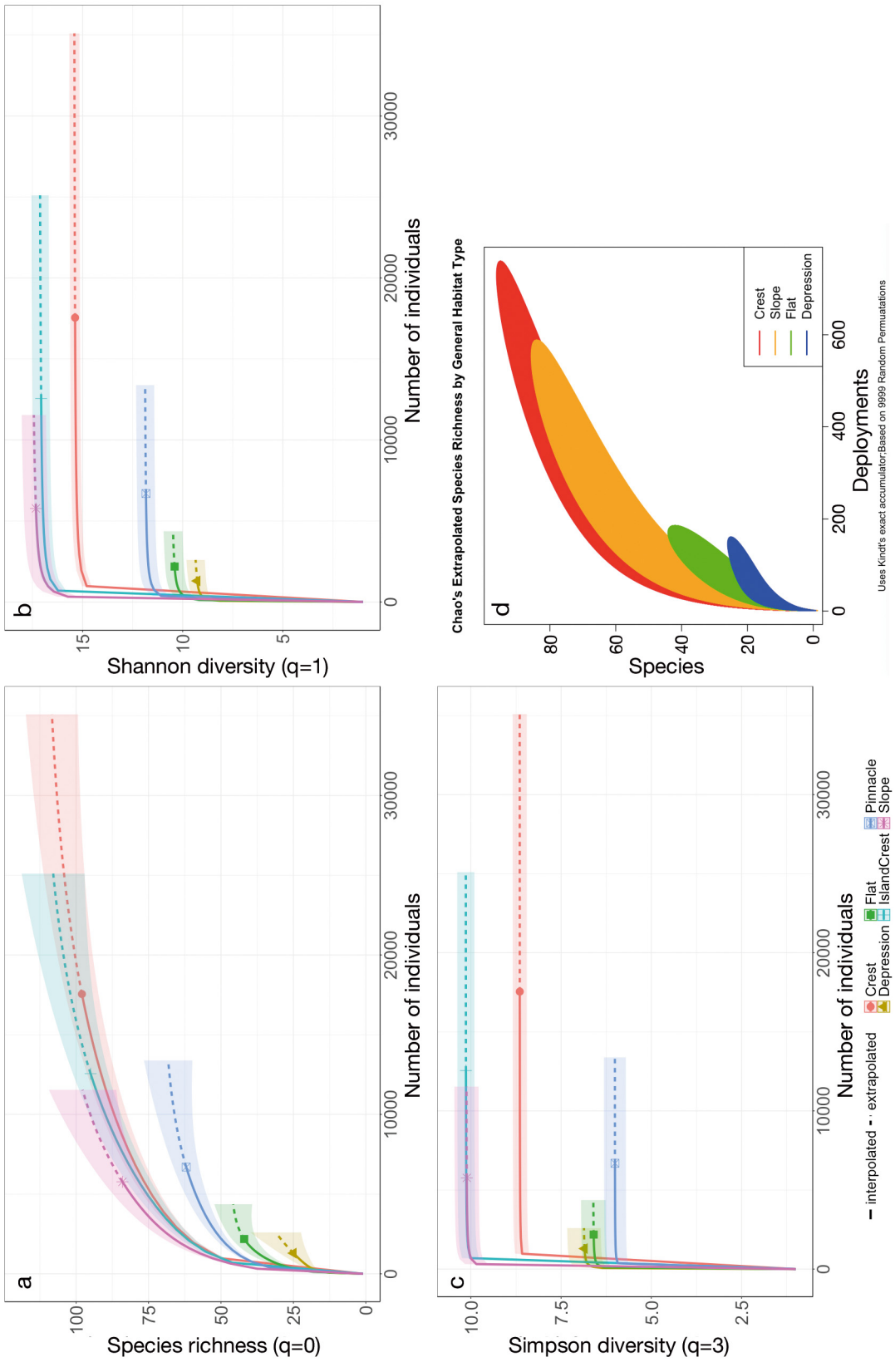

Fig. 5. Four different diversity metrics for the fish assemblage (a) species richness vs. number of individuals seen. Hill number (q = 0) based species richness interpolation (solid line) and extrapolation (dashed line) for each of the habitat types. (b) Shannon-Wiener diversity index vs. number of individuals seen. Hill number (q = 1) based Shannon-Wiener index interpolation (solid line) and extrapolation (dashed line) for each of the habitat types. (c) Simpson diversity index vs. number of individuals seen. Hill number (q = 2) based Simpson diversity index interpolation (solid line) and extrapolation (dashed line) for each of the habitat types. (d) Number of species observed vs. number of BotCam deployments. Species accumulation curves by general habitat type with 95% confidence intervals calculated using Chao index with Kindt's exact accumulator.

dissimilar habitat types were the crest habitat types and depressions or flats (overall dissimilarity: 0.9). Island crests and pinnacle assemblages were the most similar (0.81 similarity) followed closely by depression and flat assemblages. The PCoA illustrates the differences in species composition between habitat types; however, there was considerable variability between individual deployments (Figs. 6 & S3). From this analysis, we see that *P. sieboldii* and *E. coruscans* are primarily responsible for distinguishing pinnacle assemblages along with *A. rutilans* and *S. rivoliana*. In fact, *P. sieboldii* abundance on pinnacles was 2 times its abundance on island crests and over 4.8 times its abundance on any other habitat type (Table S2). Island crest assemblages are primarily distinguished from pinnacle assemblages by *P. zonatus*, which were over 5 times more abundant on island crests than pinnacles. *Hyporthodus quernus*, *P. filamentosus*, *Aprion virescens*, and *Sufflamen fraenatum* also contributed to a lesser extent. Slope assemblages were quite similar those on crests. Differences in the abundance of *S. dumerili* were mainly responsible for driving the small differences that did exist between the habitats, though it should be noted that the relative abundance of *S. dumerili* was not highest on slope habitats. Assemblages of flats and depressions were very similar to each other and mainly distinguished from the others by the abundance of *E. carbunculus*, *S. mitsukurii*, and *Carcharhinus plumbeus*, which were all found at the highest relative abundances on flats with nearly equivalent abundances on depressions (Table S2).

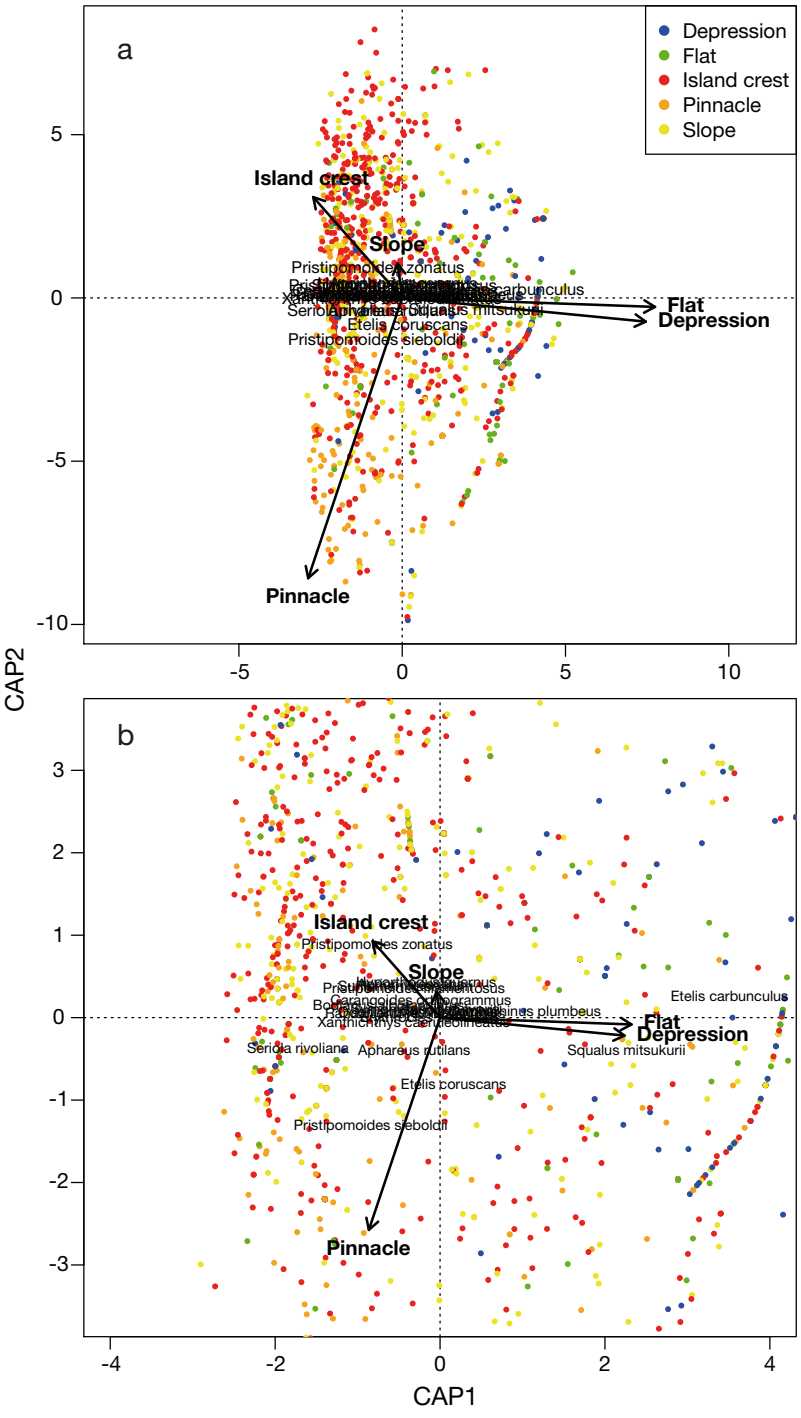

Fig. 6. Constrained principal coordinate analysis (PCoA) plots showing the relationship between deployments using data for the 20 most frequent species. Points represent deployments and are color coded by habitat. Orange and red: crests; yellow: slopes; blue: depressions; green: flats. Panels show the ordination constrained by detailed habitat types with species overlaid. Panel (b) is a focus on the origin of (a) intended to show the finer scale clustering. Species level data constrained by general habitat types is in Fig. S3. Arrows point in the direction of maximum correlation and lengths are proportional to the strength of correlation between each habitat type and the primary and secondary ordination axes ('site scores')

3.5. Current modifications by bathymetry and fish response

Time-averaged currents estimated from the ROMS model were examined around the island of Ni'ihau, which has offshore pinnacles in a range of sizes as well as all other habitat types.

Local horizontal current accelerations were found around large pinnacles and specific areas along the island shelf break (Fig. 3). The regions with the most pronounced current enhancements were promontories on the crest habitat type, both on the island shelf and those on pinnacles. Narrow channels, such as the channel between 2 large pinnacles off the southeastern coast, also show current accelerations. In general, average bottom current speed was correlated with the current amplitude (corr = 0.84) because the tidal frequency dominated the current signal. Therefore, these same areas had the largest current amplitudes as well (Fig. 7). On each pinnacle, bands of enhanced average flow speed highlight the promontories on the features rather than creating uniform flow enhancement around the features parallel to the contours. In addition to increasing current speed, mean current direction was modified by the bathymetry as seen by the convergence (Fig. 8) and the velocity quiver plots (Fig. 3). Interestingly, pinnacles and headlands along the island shelf are areas of convergence (Fig. 8).

In the waters around Ni'ihau, higher fish abundances occurred at deployments with higher mean bottom current amplitudes ($p = 0.001$), and locations where velocity vectors converge also had higher abundances ($p = 0.056$, total explained deviance = 26%; Fig. 9). Because convergent bottom flows result in upward vertical flow, areas of convergent flows are consequently sites of upwelling. Therefore, convergence also signals fish attraction to areas of localized upwelling. Pinnacles also supported significantly higher fish abundances off Ni'ihau, whereas island crests did not, and this pattern is likely largely driven by the southern island crest area, which had both low flow speeds and very low fish abundances. Our modeling efforts have revealed that enhanced current amplitudes due to bathymetric steering and areas of convergence are associated with an increase in bottomfish abundances.

4. DISCUSSION

Large-scale bathymetric habitats play an important role in structuring demersal fish assemblages across the MHI. We have shown that different habitat types have unique species compositions, with different fishes dominating in crest versus in flat/depressed habitats and slope habitats forming an intermediate, high-diversity assemblage. Crest habitats are further distinguished by hosting greater fish abundances and, through our modeling efforts, we provide evidence for a mechanistic link between these localized high abundances and bathymetrically modified hydrodynamics in these habitats.

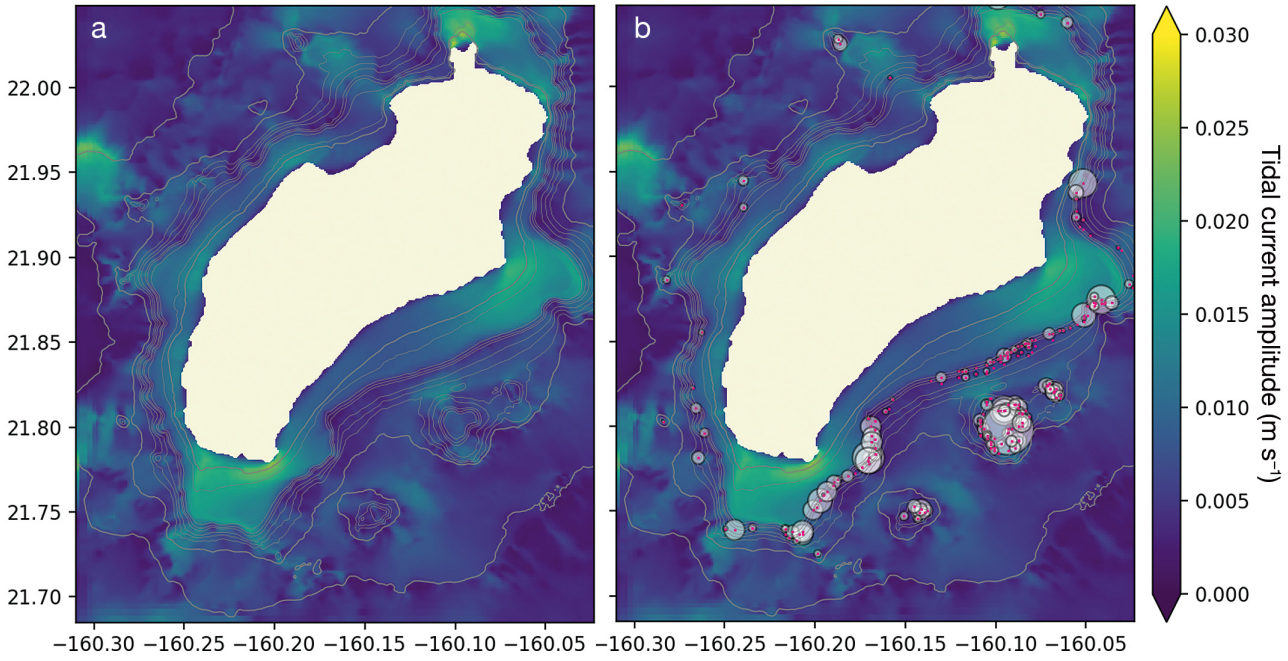

Fig. 7. Calculated mean current amplitude at the tidal frequency (mean absolute value of current speed at tidal frequency) around the island of Ni'ihau (a) without and (b) with BotCam locations (pink) where white circles are scaled to teleost MaxN and depth contours as in Fig. 3. Latitude is plotted on the *y*-axis in °N; longitude on the *x*-axis in °E

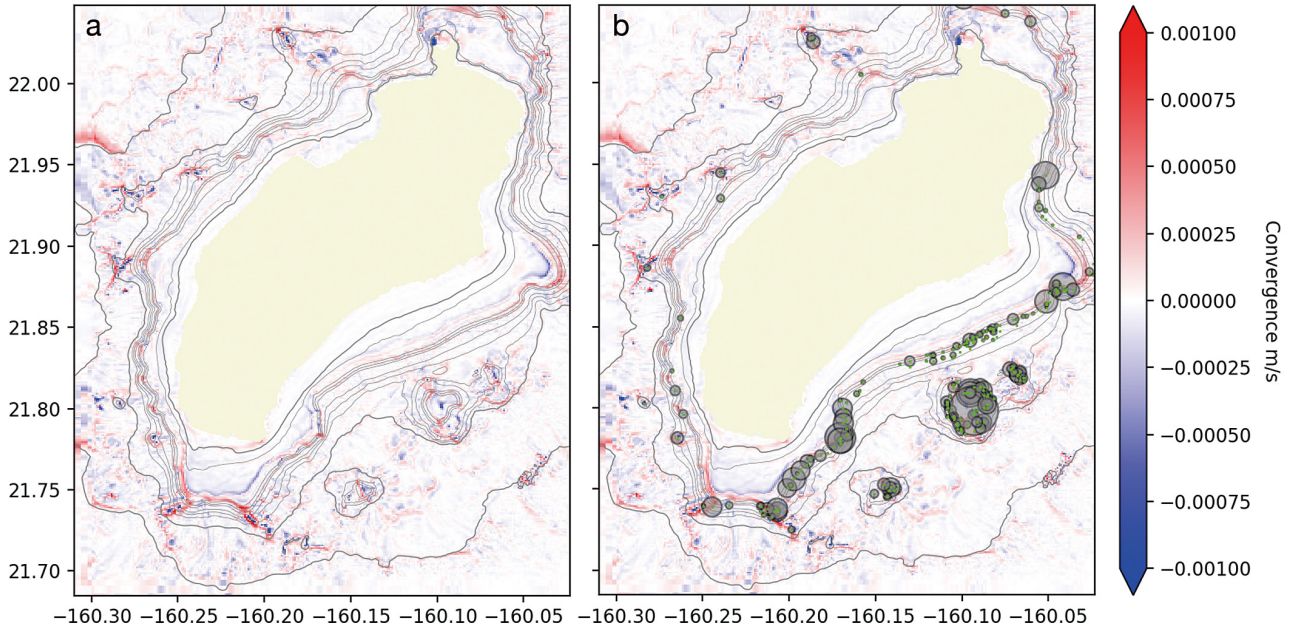

Fig. 8. Calculated current convergence $\delta w/\delta z$ (convergence is positive and in red, divergence negative and in blue) around the island of Niʻihau (a) without and (b) with (bottom) BotCam locations (green) with grey bubbles scaled to fish abundance (total teleost MaxN) and depth contours as in Fig. 3. Latitude is plotted on the *y*-axis in °N and longitude on the *x*-axis in °E

Our model results show that the formation of convergence zones and bands of high current speeds are highly localized to promontories on the shelf break and promontories on offshore pinnacles, and that high fish abundances are concentrated at these features rather than being found uniformly along the island shelf. We believe that it is the combination of flow acceleration and convergence that leads to higher abundances. Various authors have hypothesized that there may be a mechanistic link between headland and pinnacle fish aggregations and current flow (Brock & Chamberlain 1968, Ralston et al. 1986), but this idea had never before been directly tested. Bathymetric influences on current flow are an active area of research. For example, a field study on a small seamount along Kaena ridge north of Oahu found that currents were accelerated around the seamount rather than over the top (Carter et al. 2006). Our ROMS model showed similar deflection and acceleration around pinnacles, corresponding to high observed fish abundance at these sites (Fig. 9). While the high-resolution ROMS model highlighted both pinnacles and headlands along the island shelf break ('crests') as regions of enhanced flow and higher current amplitude, only pinnacles in the ROMS model domain had significantly higher fish abundances. This was due to the fact the crests habitat type included regions along the shelf break which had neither flow accelerations nor higher fish

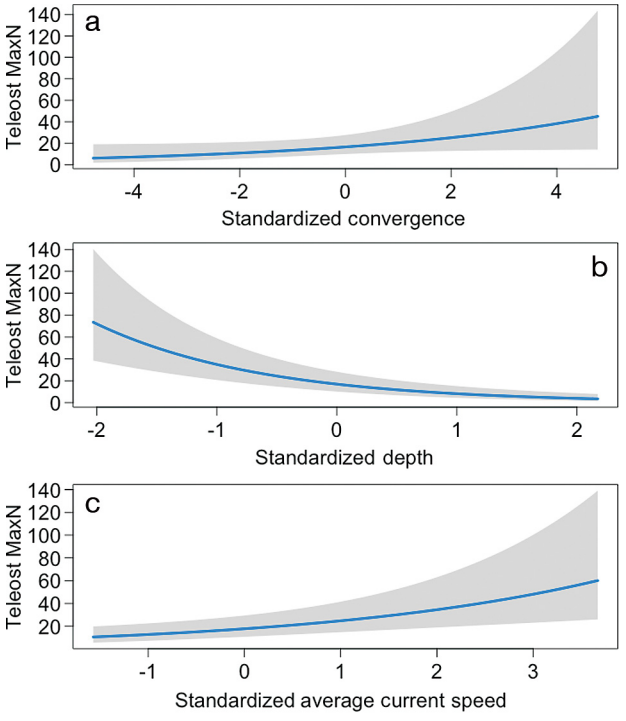

Fig. 9. Fit relationships between average current parameters and relative fish abundance (Teleost MaxN). Teleost MaxN (a) vs. depth standardized to a mean of 0 ($p \leq 0.001$), (b) vs. average bottom current speed standardized to a mean of 0 ($p \leq 0.05$), and (c) vs. convergence standardized to a mean of 0 ($p \leq 0.05$). Blue lines: estimated regression fit; gray shading: 95% confidence intervals in regression slope estimate. Plots with raw data points overlaid are in Fig. S4

abundance. This provides evidence for a link between bottom flow characteristics and demersal fish distributions.

Convergent flows have been shown to concentrate planktonic prey (Franks 1992, Hood et al. 1999), especially buoyant plankton, and the interaction of tidal currents with promontories in shallow water (headlands) can result in a zone of convergence with high concentrations of plankton (Mann & Lazier 2006, Chapter 6.7). The zonal and meridional components of the bottom currents in our model domain were heavily dominated by the tidal frequency, and it would follow that convergences in bottom currents around deep promontories and pinnacles could act in a similar way, concentrating prey items and thereby attracting predators. Moreover, because tidal currents are regular and predictable, the resulting concentrations of prey are a reliable feature of these habitats.

The interaction of the tides with crests, such as the Ni'ihau island shelf break, can also generate internal waves (Holloway & Merrifield 1999). These add energy to the mixed layer, resulting in a deepening of the mixed layer and the incorporation of nutrient-rich, cool water from below the thermocline. Additionally, the generation of the internal tide, which occurs at the sloping bottom, leads to strong mixing close to the bottom (McPhee-Shaw 2006). This strong mixing can resuspend sediments from the seafloor and entrain nutrients from those sediments into the lower few meters of the bottom, which can also act to attract lower trophic organisms (McPhee-Shaw 2006). Because this augmentation of nutrients occurs on a regular daily interval, it can result in a relatively stable increase in primary producers (if in the euphotic zone) and a corresponding enhancement in zooplankton and fish (reviewed by Mann & Lazier 2006, Chapter 6.4). In addition, internal waves can enhance aggregation of prey (Stevick et al. 2008, Embling et al. 2013). Embling et al. (2013) showed that changes in the numbers, densities, and morphologies of fish schools were related to internal wave activity. Gove et al. (2016) also suggested that a similar mechanism may contribute to the Island Mass Effect, where phytoplankton biomass increases as one approaches an island.

One could then hypothesize that this increased mixing leading to increased food availability could also be driving high fish abundances close to the island shelf. However, high fish abundances are not found uniformly along the island shelf, but rather they are concentrated at crests where currents converge and current speeds are high. This relationship with convergence may also explain the low fish abundances in depressions, where flow can be enhanced as water is squeezed horizontally through a channel but does not converge. Thus, it may be that fish do not just simply respond to increased flow, which can increase the delivery rate of plankton food to station-holding predators, but that they also respond to areas of convergence that additionally increase pelagic prey densities and nutrient concentrations (Genin 2004, Gove et al. 2019). This would make pinnacles and promontories ideal habitats for predators, especially pelagic predators, in comparison to depressions like canyons, which have enhanced detrital inputs that instead fuel a benthic food web (De Leo et al. 2012).

Indeed, crest-associated species are generally pelagic predators, while those associated with flats and depressions are benthic predators. Many of the species most dominant in crest habitats feed on pelagic prey, for example, *Aphareus rutilans*, *Aprion virescens*, *Etelis coruscans*, *Pristipomoides filamentosus*, *P. sieboldii*, and *Seriola rivoliana* (Haight et al. 1993b, Kelley & Moriwake 2012). Moreover, 2 of the 3 most influential flat-associated species, *Squalus mitsukurii* and *Carcharhinus plumbeus*, rely mostly on benthic prey (Kelley & Moriwake 2012). In the case of *C. plumbeus* (sandbar shark), its association with flats and depressions has been noted in previous studies, and in this study may reflect the distribution of *S. mitsukurii*, a frequent prey item for sandbar sharks (Musick et al. 2009). *E. carbunculus* was also most frequently found on flats and depressions and was identified as the most influential species driving the differences between assemblages of flat habitats and other habitat types, and this species is known to feed primarily on benthic fishes and crustaceans (Kelley & Moriwake 2012, Sackett et al. 2015). Previous habitat observations on this species has also noted a preference for flat, hard substrate (Misa et al. 2013). However, this ecological explanation for the noted distributions does not hold for all species. For example, *Hyporthodus quernus* is almost exclusively a benthic piscivore yet was found to be associated with crests both in this study and in previous studies of this species (Oyafuso et al. 2017). Nevertheless, stable isotope analyses have shown that while all bottomfish rely to some extent on the benthic food web, each species also feeds on pelagic prey to varying degrees and so could still derive some benefit from increased pelagic prey flux and enhanced densities resulting from flow conditions at crests (Sackett et al. 2015). For example, the prey of a benthic carnivore may be dependent on adequate availability of

pelagic prey such that even a benthic predator such as *H. quernus* would benefit from a habitat that supports higher abundances of pelagic prey items.

However, a species' ideal habitat is shaped by more than just food availability (Crowder & Cooper 1982). Our statistical models, like nearly all habitat-modeling studies, have shown the importance of depth, whose effect is likely a combination of temperature and light gradients. For example, Kelley et al. (2006) documented a distinct faunal assemblage shift at the family level in the Northwestern Hawaiian Islands at depths between 100 and 400 m. *P. filamentosus* and *A. rutilans* are predominantly found above 200 m, while *E. carbunculus* and *E. coruscans* are mostly found in deeper waters (Misa et al. 2013). This can be expected, as different species have different physiological tolerances and metabolic requirements that structure fish populations in the vertical dimension (Drazen & Seibel 2007, Drazen & Haedrich 2012). While these ideas may explain the importance of depth in structuring the fish assemblage over the different habitat types, they do not help to explain the strong preference found for crest habitats.

Another consideration that must be made when speaking about habitat preferences is that of predation. While the most influential species are all predators, some, like *E. carbunculus*, are vulnerable to predation by larger bottomfish such as *Seriola* spp. or sharks (Kelley & Moriwake 2012). One strategy to avoid predation for vulnerable species would be to avoid those habitats where potential predator densities are generally higher, such as crests. Therefore, the habitat associations for some species may be driven more by predator avoidance than by prey distribution (Werner et al. 1983, Helfman 1989).

Though we focused primarily on large-scale habitat types, micro-scale habitat can also play an important role, especially for predator avoidance (Kelley et al. 2006). For example, vulnerable species require shelter in the form of small cavities and complex bottom structures, which may be the most important feature for them (Crowder & Cooper 1982, Werner et al. 1983, Kelley et al. 2006). Island crests and pinnacles are often structurally complex at both the mega and micro scale (Scanlon et al. 2003, Kelley et al. 2006) and may be a preferred habitat for such a large range of species because they afford both enhanced food availability and increased shelter from potential predators. For example, the abundance of shelter and schooling strategies may be how the relatively small and vulnerable *P. sieboldii* can remain at such high abundances on predator-rich crest habitats (Kelley & Moriwake 2012, Misa et al. 2013).

There are important implications and applications of these findings in the conservation and management spheres. Six of the 7 of the most economically valuable bottomfish species in the MHI were within the group of species most important to differentiating assemblages among habitat types, and the one not included (*H. quernus*) also showed a strong association with the crest habitat. Additionally, recent quantitative habitat modeling efforts have noted the importance of the BPI metric on the presence/absence of several of these commercially important species (Moore et al. 2016, Oyafuso et al. 2017). Our findings extend these quantitative results to the larger demersal fish assemblage and show that mega-scale habitat classifications can be an intuitive and useful way to understand fish distribution. Inclusion of broad-scale habitat classes in fisheries management efforts could be a simple way to increase the specificity of the EFH definitions for these demersal fishes. For instance, fishery-independent stock surveys and assessments could benefit by taking into account variations in fish densities between habitat categories within the management region (Ault et al. 2018). Therefore, our results can provide simple, helpful guidance for ecosystem-based management beyond the current, broad 0–400 m EFH definition (Dunlap et al. 2016). Moreover, many of these groups are commercially valuable and exploited throughout the tropical Pacific, and for many regions fine-scale bathymetry data is often lacking. The advantage of using these large-scale habitat categories is that they could potentially be applied for species and ecosystem resource management in those regions, since large-scale bathymetric habitat types can be identified without high-resolution data. In fact, our results suggest that protection of crest habitats, which have the highest fish abundance and a high diversity, may be a simple, effective, and efficient spatial management strategy for many fish species.

Acknowledgements. We thank the State of Hawai'i Division of Aquatic Resources for providing funding for the BotCam program via the Federal Aid in Sport Fish Restoration program (F17R35-study IX). We thank the Denise B. Evans Fellowships in Oceanographic Research awarded by the University of Hawai'i Department of Oceanography in 2017 for the 2018 year, which supported the lead author for one year during the data analysis phase of this project. We also thank NOAA's Pacific Islands Fisheries Sciences Center (PIFSC) and Ben Richards for their collaboration on the BotCam and gear intercalibration projects. We give credit to NOAA and SOEST for development of the bathymetry synthesis, specifically the NOAA/PIFSC Fisheries Research and Monitoring Division (FRMD), through a grant to JIMAR, for providing funding for this project. Special thanks to the BotCam crew

Virginia Moriwake, Chris Demarke, Bo Alexander, John Yeh, William Misa, Jason Friedman, Matt Waterhouse, Dana Sackett, Aharon Fleury, and Clif Nunnally for their field efforts, video analysis, and database management. We thank Professor Eric Firing for invaluable help and advice with data analysis. SOEST contribution number 11185.

LITERATURE CITED

Ault JS, Smith SG, Richards BL, Yau AJ and others (2018) Towards fishery-independent biomass estimation for Hawaiian Islands deepwater snappers. Fish Res 208: 321–328

Azevedo Correia de Souza JM, Powell BS (2017) Different approaches to model the nearshore circulation in the south shore of O'ahu, Hawaii. Ocean Sci 13:31–46

Barton K (2016) R package MuMIn: multi-model inference. R package v.1.43.17. https://CRAN.R-project.org/package=MuMIn

Benoit-Bird KJ, Battaile BC, Heppell SA, Hoover B and others (2013) Prey patch patterns predict habitat use by top marine predators with diverse foraging strategies. PLOS ONE 8:e53348

Brock VE, Chamberlain TC (1968) A geological and ecological reconnaissance off western Oahu, Hawaii, principally by means of the research submarine 'Asherah'. Pac Sci 22:373–394

Cappo M, Harvey E, Shortis M (2006) Counting and measuring fish with baited video techniques—an overview. In: Lyle JM, Furlani DM, Buxton CD (eds) Proc Australian Soc Fish Biol Workshop: cutting-edge technology in fish and fisheries science. Australian Society for Fish Biology, Hobart, p 101–114

Carter GS, Gregg MC, Merrifield MA (2006) Flow and mixing around a small seamount on Kaena Ridge, Hawaii. J Phys Oceanogr 36:1036–1052

Chambers JM, Cleveland WS, Kleiner B, Tukey PA (1983) Graphical methods for data analysis. Wadsworth & Brooks/Cole, Belmont, CA

Chao A, Gotelli NJ, Hsieh TC, Sander EL, Ma KH, Colwell RK, Ellison AM (2014) Rarefaction and extrapolation with Hill numbers: a framework for sampling and estimation in species diversity studies. Ecol Monogr 84: 45–67

Cribari-Neto F, Zeileis A (2010) Beta Regression in R. J Stat Softw 34:1–24

Crowder LB, Cooper WE (1982) Habitat structural complexity and the interaction between bluegills and their prey. Ecology 63:1802–1813

De Leo FC, Smith CR, Rowden AA, Bowden DA, Clark MR (2010) Submarine canyons: hotspots of benthic biomass and productivity in the deep sea. Proc R Soc B 277: 2783–2792

De Leo FC, Drazen JC, Vetter EW, Rowden AA, Smith CR (2012) The effects of submarine canyons and the oxygen minimum zone on deep-sea fish assemblages off Hawai'i. Deep Sea Res I 64:54–70

Drazen JC, Haedrich RL (2012) A continuum of life histories in deep-sea demersal fishes. Deep Sea Res I 61:34–42

Drazen JC, Seibel BA (2007) Depth-related trends in metabolism of benthic and benthopelagic deep-sea fishes. Limnol Oceanogr 52:2306–2316

Dunlap M, Everson A, Jayewardene D, Makaiau J, Mitsuyasu M, Pautzke S, Walker R (2016) Amendment 4 to the Fishery Ecosystem Plan for the Hawaii Archipelago. Western Pacific Regional Fishery Management Council, Honolulu, HI

Durden JM, Bett BJ, Jones DOB Huvenne VAI, Ruhl HA (2015) Abyssal hills—hidden source of increased habitat heterogeneity, benthic megafaunal biomass and diversity in the deep sea. Prog Oceanogr 137:209–218

Egbert GD, Erofeeva SY (2002) Efficient inverse modeling of barotropic ocean tides. Ocean Technol 19:183–204

Embling CB, Sharples J, Armstrong E, Palmer MR, Scott BE (2013) Fish behaviour in response to tidal variability and internal waves over a shelf sea bank. Prog Oceanogr 117: 106–117

Franks PJS (1992) Sink or swim: accumulation of biomass at fronts. Mar Ecol Prog Ser 82:1–12

Friedrich T, Timmermann A, Decloedt T, Luther DS, Mouchet A (2011) The effect of topography-enhanced diapycnal mixing on ocean and atmospheric circulation and marine biogeochemistry. Ocean Model 39:262–274

Genin A (2004) Bio-physical coupling in the formation of zooplankton and fish aggregations over abrupt topographies. J Mar Syst 50:3–20

Genin A, Jaffe JS, Reef R, Richter C, Franks PJS (2005) Swimming against the flow: a mechanism of zooplankton aggregation. Science 308:860–862

Gove JM, McManus MA, Neuheimer AB, Polovina JJ and others (2016) Ocean oases: near-island biological hotspots in barren ocean basins. Nat Commun 7:10581

Gove JM, Whitney JL, McManus MA, Lecky J and others (2019) Prey-size plastics are invading larval fish nurseries. Proc Natl Acad Sci USA 116:24143–24149

Haight WR, Kobayashi DR, Kawamoto KE (1993a) Biology and management of deepwater snappers of the Hawaiian Archipelago. Mar Fish Rev 55:20–27

Haight WR, Parrish JD, Hayes TA (1993b) Feeding ecology of deepwater lutjanid snappers at Penguin Bank, Hawaii. Trans Am Fish Soc 122:328–347

Harris PT, Macmillan-Lawler M, Rupp J, Baker EK (2014) Geomorphology of the oceans. Mar Geol 352:4–24

Helfman GS (1989) Threat-sensitive predator avoidance in damselfish–trumpetfish interactions. Behav Ecol Sociobiol 24:47–58

Holloway PE, Merrifield MA (1999) Internal tide generation by seamounts, ridges, and islands. J Geophys Res 104: 25937–25951

Hood RR, Wang HV, Purcell JE, Houde ED, Harding LW (1999) Modeling particles and pelagic organisms in Chesapeake Bay: convergent features control plankton distributions. J Geophys Res 104:1223–1243

Hsieh TC, Ma KH, Chao A (2016) INEXT: an R package for rarefaction and extrapolation of species diversity (Hill numbers). Methods Ecol Evol 7:1451–1456

Ichino MC, Clark MR, Drazen JC, Jamieson A and others (2015) The distribution of benthic biomass in hadal trenches: a modelling approach to investigate the effect of vertical and lateral organic matter transport to the seafloor. Deep Sea Res I 100:21–33

Jamieson AJJ, Kilgallen NM, Rowden AA, Fujii T and others (2011) Bait-attending fauna of the Kermadec Trench, SW Pacific Ocean: evidence for an ecotone across the abyssal-hadal transition zone. Deep Sea Res I 58:49–62

Janeković I, Powell BS, Matthews D, McManus MA, Sevadjian JC (2013) 4D-var data assimilation in a nested, coastal ocean model: a Hawaiian case study. J Geophys Res 118:5022–5035

Kelley CD, Moriwake VN (2012) Appendix 3: essential fish habitat descriptions for Western Pacific archipelagic and remote island areas fishery ecosystem plan management unit species. Part 1: bottomfish. Western Pacific Regional Fishery Management Council, Honolulu, HI

Kelley C, Moffitt R, Smith JR (2006) Mega-to micro-scale classification and description of bottomfish essential fish habitat on four banks in the Northwestern Hawaiian Islands. Atoll Res Bull 543:319–332

Lueck RG (1997) Topographically induced mixing around a shallow seamount. Science 276:1831–1833

Lundblad ER, Wright DJ, Miller J, Larkin EM and others (2006) A benthic terrain classification scheme for American Samoa. Mar Geod 29:89–111

Mann KH, Lazier JR (2006) Dynamics of marine ecosystems, 3rd edn. Blackwell Publishing, Malden, MA

Matthews D, Powell BS, Janeković I (2012) Analysis of four-dimensional variational state estimation of the Hawaiian waters. J Geophys Res 117:C03013

McPhee-Shaw E (2006) Boundary–interior exchange: reviewing the idea that internal-wave mixing enhances lateral dispersal near continental margins. Deep Sea Res II 53:42–59

Merritt D, Donovan MK, Kelley C, Waterhouse L, Parke M, Wong K, Drazen JC (2011) BotCam: a baited camera system for nonextractive monitoring of bottomfish species. Fish Bull 109:56–67

Misa WFXE, Drazen JCJ, Kelley CD, Moriwake VN (2013) Establishing species–habitat associations for 4 eteline snappers with the use of a baited stereo-video camera system. Fish Bull 111:293–308

Misa WFXE, Richards BL, DiNardo GT, Kelley CD, Moriwake VN, Drazen JC (2016) Evaluating the effect of soak time on bottomfish abundance and length data from stereo-video surveys. J Exp Mar Biol Ecol 479:20–34

Moore CH, Harvey ES, Van Niel KP (2009) Spatial prediction of demersal fish distributions: enhancing our understanding of species–environment relationships. ICES J Mar Sci 66:2068–2075

Moore CH, Drazen JC, Kelley CD, Misa WFXE (2013) Deep-water marine protected areas of the main Hawaiian Islands: establishing baselines for commercially valuable bottomfish populations. Mar Ecol Prog Ser 476:167–183

Moore C, Drazen JC, Radford BT, Kelley C, Newman SJ (2016) Improving essential fish habitat designation to support sustainable ecosystem-based fisheries management. Mar Policy 69:32–41

Morato T, Hoyle SD, Allain V, Nicol SJ (2010) Seamounts are hotspots of pelagic biodiversity in the open ocean. Proc Natl Acad Sci USA 107:9707–9711

Morris KJ, Bett BJ, Durden JM, Benoist NMA and others (2016) Landscape-scale spatial heterogeneity in phytodetrital cover and megafauna biomass in the abyss links to modest topographic variation. Sci Rep 6:34080

Musick JA, Stevens JD, Baum JK, Bradai M and others (2009) *Carcharhinus plumbeus* (sandbar shark). The IUCN Red List Of Threatened Species 2009: eT3853A10130397. https://dx.doi.org/10.2305/IUCN.UK.2009-2.RLTS.T3853A10130397.en

Oksanen J, Blanchet FG, Kindt R, Legendre P and others (2015) vegan: community ecology package. 2.5-6. https://github.com/vegandevs/vegan

Oyafuso ZS, Drazen JC, Moore CH, Franklin EC (2017) Habitat-based species distribution modelling of the Hawaiian deepwater snapper–grouper complex. Fish Res 195:19–27

Pacific Islands Fisheries Science Center (2020) Multi beam bathymetry and backscatter synthesis for the Main Hawaiian Islands (5 meter resolution) from 2010-06-15 to 2010-08-15. https://inport.nmfs.noaa.gov/inport/item/31636

Parke M (2007) Linking Hawaii fisherman reported commercial bottomfish catch data to potential bottomfish habitat and proposed restricted fishing areas using GIS and spatial analysis. NOAA Tech Memo NMFS-PIFSC-11

Partridge D, Friedrich T, Powell BS (2019) Reanalysis of the PacIOOS Hawaiian Island ocean forecast system, an implementation of the Regional Ocean Modeling System v3.6. Geosci Model Dev 12:195–213

Pingree RD, Pugh PR, Holligan PM, Forster GR (1975) Summer phytoplankton blooms and red tides along tidal fronts in the approaches to the English Channel. Nature 258:672–677

Pitcher TJ, Morato T, Hart PJB, Clark MR, Haggan N, Santos RS (eds) (2007) Seamounts: ecology, fisheries and conservation. Blackwell Fisheries and Aquatic Resources Series, Vol 12. Blackwell Publishing, Oxford

Polovina JJ, Howell E, Kobayashi DR, Seki MP (2001) The transition zone chlorophyll front, a dynamic global feature defining migration and forage habitat for marine resources. Prog Oceanogr 49:469–483

Powell BS (2017) Quantifying how observations inform a numerical reanalysis of Hawaii. J Geophys Res 122: 427–444

Priede IG, Bagley PM, Smith A, Creasey S, Merrett NR (1994) Scavenging deep demersal fishes of the Porcupine Seabight, north-east Atlantic: observations by baited camera, trap and trawl. J Mar Biol Assoc UK 74:481–498

R Core Team (2018) R: a language and environment for statistical computing. R Foundation for Statistical Computing, Vienna

Ralston S, Gooding RM, Ludwig GM (1986) An ecological survey and comparison of bottom fish resource assessments (submersible versus handline fishing) at Johnston Atoll. Fish Bull 84:141–156

Richards BL, Smith JR, Smith SG, Ault JS, Kelley CD, Moriwake VN (2019) Development and use of a novel Main Hawaiian Islands bathymetric and backscatter synthesis in a stratified fishery-independent bottomfish survey. NOAA Tech Memo NMFS-PIFSC-87

Rudnick DL, Boyd TJ, Brainard RE, Carter GS and others (2003) From tides to mixing along the Hawaiian Ridge. Science 301:355–357

Sackett DK, Drazen JC, Moriwake VN, Kelley CD, Schumacher BD, Misa WFXE (2014) Marine protected areas for deepwater fish populations: an evaluation of their effects in Hawai'i. Mar Biol 161:411–425

Sackett DK, Drazen JC, Choy CA, Popp B, Pitz GL (2015) Mercury sources and trophic ecology for Hawaiian bottomfish. Environ Sci Technol 49:6909–6918

Sackett DK, Kelley CD, Drazen JC (2017) Spilling over deepwater boundaries: evidence of spillover from two deepwater restricted fishing areas in Hawaii. Mar Ecol Prog Ser 568:175–190

Scanlon K, Koenig C, Coleman F, Miller M (2003) Importance of geology to fisheries management: examples from the northeastern Gulf of Mexico. Am Fish Soc Symp 36:95–99

Shchepetkin AF, McWilliams JC (2003) A method for computing horizontal pressure-gradient force in an oceanic model with a nonaligned vertical coordinate. J Geophys Res 108:3090

Shchepetkin AF, McWilliams JC (2005) The Regional Ocean Modeling System: a split-explicit, free-surface, topography following coordinates ocean model. Ocean Model 9: 347–404

Smith JR (2016) Multibeam backscatter and bathymetry synthesis for the Main Hawaiian Islands. Final technical report July 2016. Hawaii Undersea Research Laboratory, Honolulu, HI

Stevick PT, Incze LS, Kraus SD, Rosen S, Wolff N, Baukus A (2008) Trophic relationships and oceanography on and around a small offshore bank. Mar Ecol Prog Ser 363:15–28

Sutton TT, Porteiro FM, Heino M, Byrkjedal I and others (2008) Vertical structure, biomass and topographic association of deep-pelagic fishes in relation to a mid-ocean ridge system. Deep Sea Res II 55:161–184

Turnewitsch R, Falahat S, Nycander J, Dale A, Scott RB, Furnival D (2013) Deep-sea fluid and sediment dynamics — influence of hill- to seamount-scale seafloor topography. Earth-Science Rev 127:203–241

Vetter EW, Dayton PK (1999) Organic enrichment by macrophyte detritus, and abundance patterns of megafaunal populations in submarine canyons. Mar Ecol Prog Ser 186:137–148

Werner EE, Gilliam JF, Hall DJ, Mittelbach GG (1983) An experimental test of the effects of predation risk on habitat use in fish. Ecology 64:1540–1548

Wessel P, Sandwell DT, Kim SS (2010) The global seamount census. Oceanography (Wash DC) 23:24–33

Wong-Ala JATK, Comfort CM, Gove JM, Hixon MA and others (2018) How life history characteristics and environmental forcing shape settlement success of coral reef fishes. Front Mar Sci 5:65

Wright DJ, Pendleton M, Boulware J, Walbridge S and others (2012) ArcGIS Benthic Terrain Modeler (BTM), v. 3.0. ESRI, Redlands, CA

Zuur AF, Ieno EN, Elphick CS (2010) A protocol for data exploration to avoid common statistical problems. Methods Ecol Evol 1:3–14

Editorial responsibility: Jana Davis, Annapolis, Maryland, USA
Reviewed by: T. Lorraine Sih and 2 anonymous referees

Submitted: May 6, 2020
Accepted: November 12, 2020
Proofs received from author(s): January 22, 2021